AD-A074 429 OHIO STATE UNIV COLUMBUS ELECTROSCIENCE LAB F/G 9/5
POWER OPTIMIZATION IN ADAPTIVE ARRAY: A TECHNIQUE FOR INTERFERE--ETC(U)
JUL 79 R T COMPTON N00019-79-C-0281
UNCLASSIFIED ESL-711847-2 NL

| OF |
AD-
A074429

END
DATE
FILMED
11 79
DDC

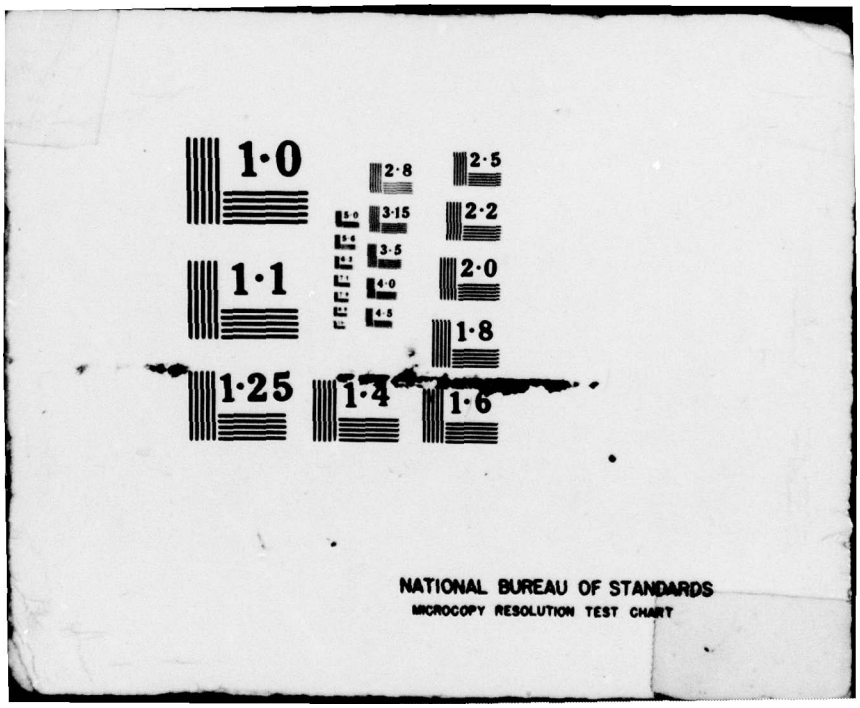
1·0
1·1
1·25
2·8
3·15
3·5
4·0
4·5
1·4
2·5
2·2
2·0
1·8
1·6
NATIONAL BUREAU OF STANDARDS
MICROCOPY RESOLUTION TEST CHART

OSU

The Ohio State University

# POWER OPTIMIZATION IN ADAPTIVE ARRAYS: A Technique for Interference Protection

R. T. Compton, Jr.

(12)

LEVEL II



The Ohio State University

**ElectroScience Laboratory**

Department of Electrical Engineering
Columbus, Ohio 43212

Technical Report 711847-2

Contract N00019-79-C-0281

July 1979



Department of the Navy
Naval Air Systems Command
Washington, D.C. 20361

## NOTICES

When Government drawings, specifications, or other data are used for any purpose other than in connection with a definitely related Government procurement operation, the United States Government thereby incurs no responsibility nor any obligation whatsoever, and the fact that the Government may have formulated, furnished, or in any way supplied the said drawings, specifications, or other data, is not to be regarded by implication or otherwise as in any manner licensing the holder or any other person or corporation, or conveying any rights or permission to manufacture, use, or sell any patented invention that may in any way be related thereto.

SECURITY CLASSIFICATION OF THIS PAGE *(When Data Entered)*

## REPORT DOCUMENTATION PAGE

READ INSTRUCTIONS BEFORE COMPLETING FORM

| | |
|---|---|
| 1. REPORT NUMBER | 2. GOVT ACCESSION NO. / 3. RECIPIENT'S CATALOG NUMBER |
| 4. TITLE *(and Subtitle)*: POWER OPTIMIZATION IN ADAPTIVE ARRAYS: A Technique for Interference Protection | 5. TYPE OF REPORT & PERIOD COVERED: Technical Report |
| | 6. PERFORMING ORG. REPORT NUMBER: ESL-711847-2 |
| 7. AUTHOR(s): R. T. Compton, Jr. | 8. CONTRACT OR GRANT NUMBER(s): Contract N00019-79-C-0281 |
| 9. PERFORMING ORGANIZATION NAME AND ADDRESS: The Ohio State University ElectroScience Laboratory, Department of Electrical Engineering, Columbus, Ohio 43212 | 10. PROGRAM ELEMENT, PROJECT, TASK AREA & WORK UNIT NUMBERS: Project N00019-79-PR-RJ006 |
| 11. CONTROLLING OFFICE NAME AND ADDRESS: Department of the Navy, Naval Air Systems Command, Washington, D.C. 20361 | 12. REPORT DATE: July 1979 / 13. NUMBER OF PAGES: 28 |
| 14. MONITORING AGENCY NAME & ADDRESS *(if different from Controlling Office)* | 15. SECURITY CLASS. *(of this report)*: Unclassified / 15a. DECLASSIFICATION/DOWNGRADING SCHEDULE |

16. DISTRIBUTION STATEMENT *(of this Report)*

**APPROVED FOR PUBLIC RELEASE: DISTRIBUTION UNLIMITED**

17. DISTRIBUTION STATEMENT *(of the abstract entered in Block 20, if different from Report)*

18. SUPPLEMENTARY NOTES



19. KEY WORDS *(Continue on reverse side if necessary and identify by block number)*

Adaptive Arrays
Antennas
Interference

20. ABSTRACT *(Continue on reverse side if necessary and identify by block number)*

This report describes a weight control algorithm that may be used in a 2-element adaptive array to protect a desired signal from an interference signal. The algorithm is a constrained gradient technique that either maximizes or minimizes array output power. It is shown that by choosing appropriately between minimization and maximization, a useful desired signal-to-interference-plus-noise ratio can be maintained at the array output over a wide range of signal powers.

DD FORM 1 JAN 73 1473 EDITION OF 1 NOV 65 IS OBSOLETE

SECURITY CLASSIFICATION OF THIS PAGE *(When Data Entered)*

402 251

CONTENTS

## INTRODUCTION

In a recent paper[1], the author described the power inversion adaptive array. Power inversion refers to the ability of an adaptive array based on the Howells-Applebaum feedback loop[2,3] to invert the power ratio of two incoming signals. It does this by nulling the strong signal in favor of the weak one. This technique can be used to protect a weak desired signal from a strong interference signal. An appealing feature of this technique is that the designer does not have to know the desired signal arrival angle or waveform in advance.

In this paper we describe a different weight control algorithm that may be used for the same purpose. As will be shown, this algorithm appears to offer slightly better performance than the power inversion array. The new algorithm either maximizes or minimizes the array output power, subject to a constraint on the weights. We refer to it as a power optimization algorithm.

The same algorithm has been described in an earlier paper[4], where it was used for a different purpose -- to obtain maximum gain from an array. In this paper we show how it may be used with a 2-element array to protect a desired signal from an interfering signal.

## THE POWER OPTIMIZING ALGORITHM

Consider a two element array of isotropic elements as shown in Figure 1. Assume the elements are spaced one-half wavelength apart at the

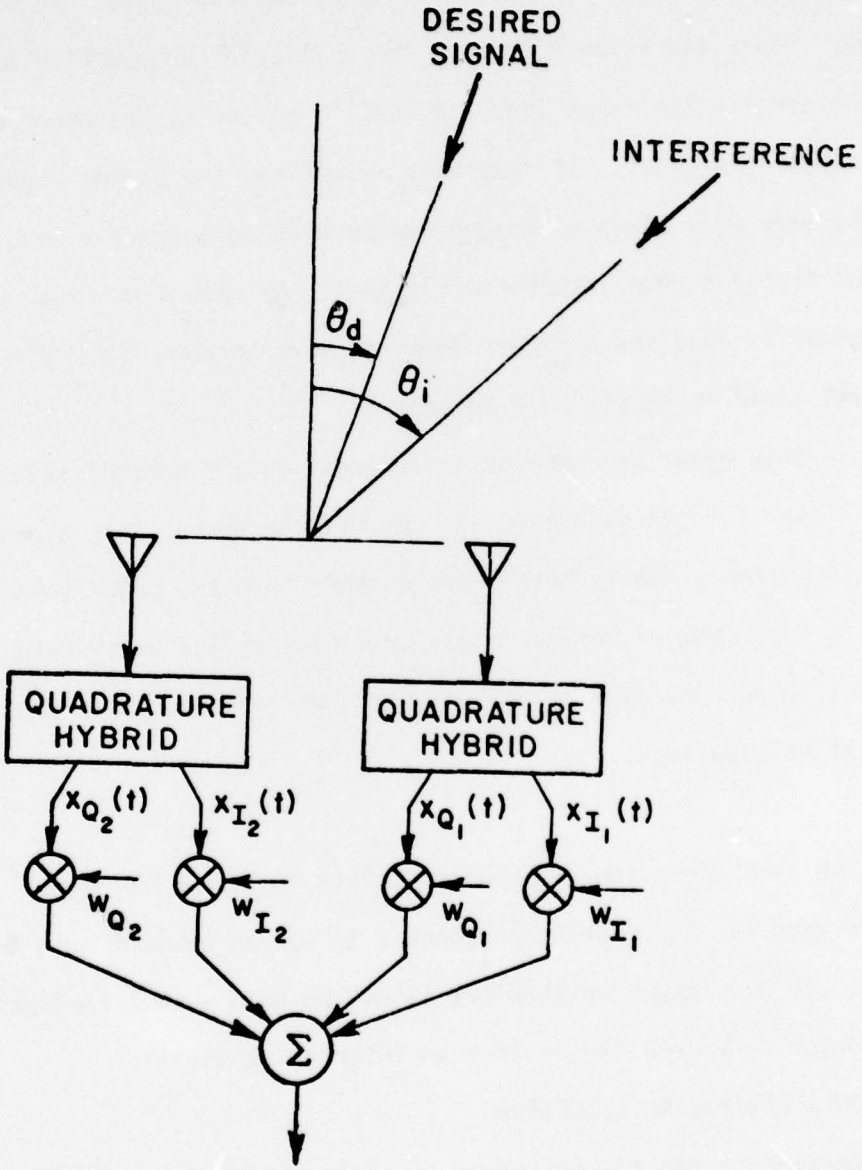


Figure 1. Two Element Adaptive Array

center frequency of the signals to be received. The signal from each element is split with a quadrature hybrid into an in-phase component $x_{I_i}(t)$ and a quadrature component $x_{Q_i}(t)$. Each of these signals is multiplied by real-valued weights $w_{I_i}$ and $w_{Q_i}$ and then summed to produce the array output signal s(t).

We assume that two signals are incident on the array, one a desired signal and the other interference. In order to protect the desired signal from the interference, we adjust the weights $w_{I_i}$, $w_{Q_i}$ either to maximize or to minimize the array output power $E\{s^2(t)\}$. ($E\{\cdot\}$ denotes the expectation.) We do this subject to the constraint that

$$\sum_{i=1}^{2} (w_{I_i}^2 + w_{Q_i}^2) = 1 \qquad (1)$$

so the weights cannot all go to zero or infinity. When the desired signal is stronger than the interference, we will maximize $E\{s^2(t)\}$. Maximizing $E\{s^2(t)\}$ causes the array to point its beam maximum toward the desired signal. When the desired signal is weaker than the interference, we will minimize $E\{s^2(t)\}$. Minimizing $E\{s^2(t)\}$ causes the array to devote its only available null* to the interference signal. In this way a useful desired signal-to-interference-plus-noise ratio (SINR) can be maintained at the array output.

An algorithm for determining weights $w_{I_i}$, $w_{Q_i}$ that maximize $E\{s^2(t)\}$, subject to the constraints in Equation (1), has been described in Reference 4. If the weights and the signals are sampled at times

---

*A two-element array has only one degree of freedom.

$$t_j = j\Delta t, \quad j=0,1,2,\ldots, \tag{2}$$

the array output power may be maximized by adjusting the weights with the iterative equation*:

$$w_{P_i}(t_{j+1}) = w_{P_i}(t_j)+k\, s(t_j)\left[x_{P_i}(t_j)-w_{P_i}(t_j)s(t_j)\right], \quad i=1,2. \tag{3}$$

Here P denotes I or Q, and k is a positive constant controlling the rate of convergence of the weights. Equation (3) determines $w_{P_i}$ at time $t_{j+1}$ from its value and the values of the signals at time $t_j$. This calculation is repeated iteratively until the weights have converged to their final values, which yield maximum array output power.

Alternatively, the algorithm in Equation (3) can be implemented in the form of a continuous control loop as shown in Figure 2. One such loop would be required for each quadrature channel in the array.

The algorithm in Equation (3) is based on a steepest-ascent maximization of $E\{s^2(t)\}$ subject to the constraint in Equation (1). The correction term $s(t_j)\left[x_{P_i}(t_j)-w_{P_i}(t_j)s(t_j)\right]$ is obtained by computing the gradient of $E\{s^2(t)\}$ and retaining only its component parallel to the weight hypersphere in Equation (1). With $k>0$ the weights then move toward a set of values that yield maximum $E\{s^2(t)\}$.

We note, however, that we may also use the same algorithm to minimize $E\{s^2(t)\}$, merely by choosing $k<0$. With $k<0$ the weights move in the constrained steepest-descent direction toward minimum $E\{s^2(t)\}$. To change from weights that maximize $E\{s^2(t)\}$ to ones that minimize $E\{s^2(t)\}$, we need only change the sign of k.

---

*This is Equation (17) of Reference 4.

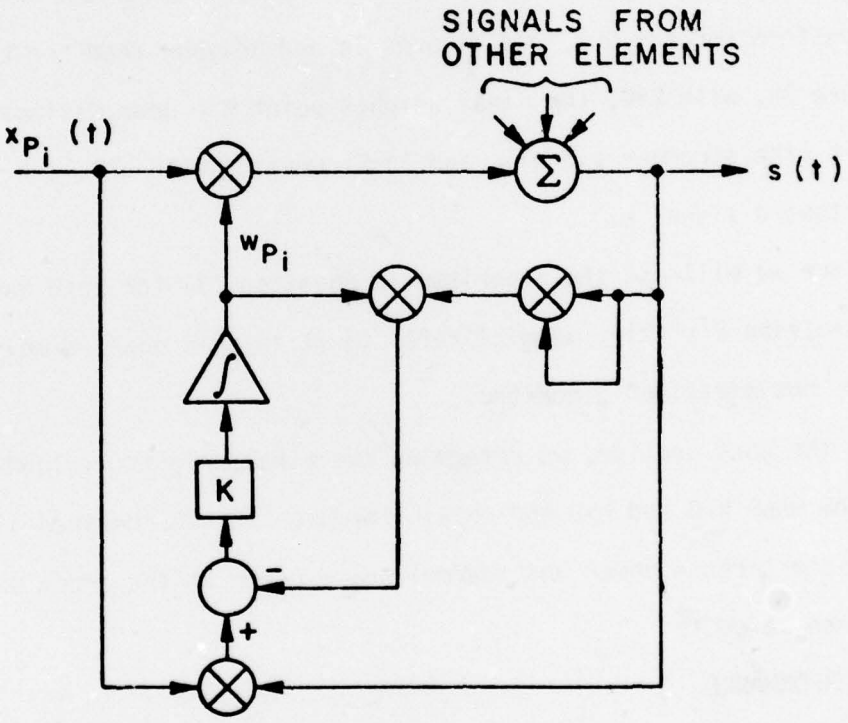


Figure 2. Continuous Gain Optimization Loop.

To illustrate this behavior, Figure 3 shows some typical weight transients and the associated final pattern for k>0 and k<0. In this figure, two signals are incident on the array, and thermal noise is also present (statistically independent between elements). Signal 1 arrives from broadside with a signal-to-noise ratio (SNR) of 10 dB per element, and Signal 2 arrives from $30^{o}$ off broadside with an SNR of 20 dB per element. Figures 3a and 3b show the weight transient and the final pattern for k=+.001, and Figures 3c and 3d show them for k=-.001. In Figure 3b, with k>0, the final weights point the beam maximum toward Signal 2 (the stronger signal), and in Figure 3d, with k<0, they point a null toward signal 2.

Since we will use the algorithm in Equation (3) for both maximizing and minimizing $E\{s^2(t)\}$, we will refer to it in this paper simply as a power "optimization" algorithm.

In the next section, we determine the final weights yielded by this algorithm when k<0 and k>0 and obtain formulas for the desired signal power, interference power and thermal noise power at the array output with these weights.

ARRAY PERFORMANCE

To study the performance of the gain optimizing algorithm, it will simplify matters if we first convert the algorithm in Equation (3) into complex form. We suppose the quadrature hybrids in Figure 1 are ideal, so that

$$x_{Q_i}(t) = \hat{x}_{I_i}(t), \quad i=1,2 \quad , \tag{4}$$

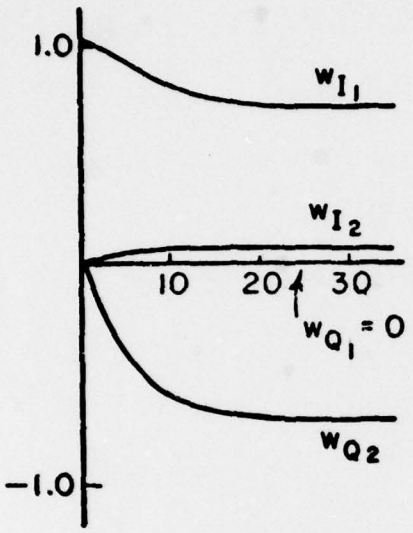


(a) Transients: k=+.001

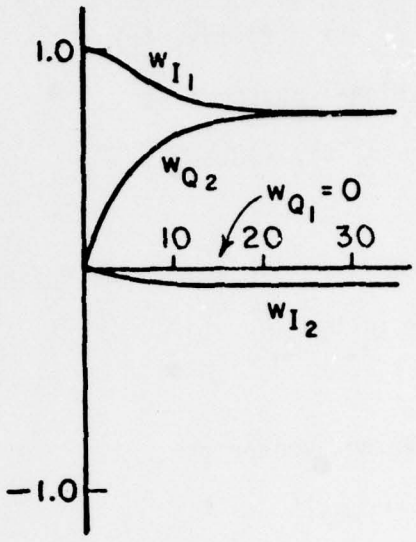


(c) Transients: k=-.001

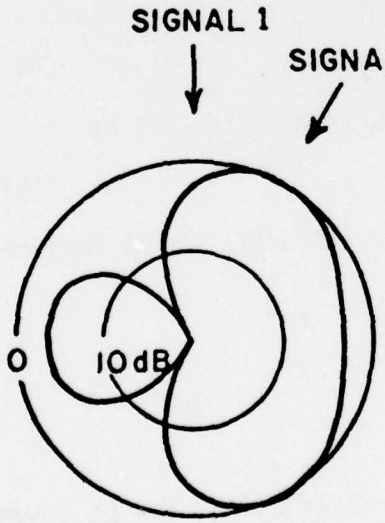


(b) Final Pattern: k=+.001

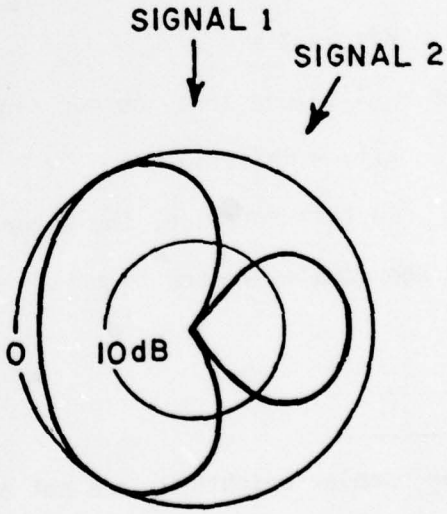


(d) Final Pattern: k=-.001

Figure 3. Typical Weight Transients and Final Patterns.

where "$\hat{}$" denotes the Hilbert Transform[5]. We define the analytic signal $\tilde{x}_i(t)$ associated with the ith element as

$$\tilde{x}_i(t) = x_{I_i}(t) + jx_{Q_i}(t)$$
$$= x_{I_i}(t) + j\hat{x}_{I_i}(t). \quad (5)$$

and the signal vector X as

$$X = (\tilde{x}_1(t), \tilde{x}_2(t))^T \quad (6)$$

(T denotes the transpose.) We define the ith complex weight as

$$w_i = w_{I_i} - jw_{Q_i} \quad (7)$$

and the weight vector as

$$w = (w_1, w_2)^T. \quad (8)$$

The analytic signal $\tilde{s}(t)$ at the array output is then*

$$\tilde{s}(t) = X^T w = w^T X \quad (9)$$

The real-valued array output signal $s(t)$ is related to $\tilde{s}(t)$ by

$$s(t) = \mathrm{Re}\{\tilde{s}(t)\} \quad (10)$$

In this notation, the algorithm in Equation (3) may be replaced by the complex vector form

---

*The complex weights $w_i$ are not analytic in general, but may be assumed bandlimited about zero frequency. The signals $\tilde{x}_i(t)$ are narrowband processes centered at a carrier frequency $\omega_0$. $\tilde{s}(t)$ will then be analytic as long as the highest frequency component in w is less than the lowest frequency component in X, which we assume to be the case.

$$w(t_{j+1}) = w(t_j) + k\tilde{s}(t_j)\left[X^*(t_j) - w(t_j)\tilde{s}^*(t_j)\right], \tag{11}$$

the use of which will simplify the derivations to follow. ("*" denotes complex conjugate.).

This algorithm will be used to control the array weights, either with $k>0$ or with $k<0$. In either case, the steady-state weights that result can be obtained by noting that, when the weights have reached their final values, which we denote by $w=w_f$, the correction term in Equation (11) must have an average value equal to zero:

$$E\{\tilde{s}\left[X^*-w_f\tilde{s}^*\right]\} = 0. \tag{12}$$

However, this may be written

$$E\{\left[X^*-w_f\tilde{s}^*\right]\tilde{s}\} = E\{X^*X^T\}w_f - E\{\tilde{s}^*\tilde{s}\}w_f = 0. \tag{13}$$

Let us denote the covariance matrix $E\{X^*X^T\}$ by

$$\Phi = E\{X^*X^T\}, \tag{14}$$

and also note that $E\{\tilde{s}^*\tilde{s}\}$ is scalar. Thus $w_f$ satisfies

$$\Phi w_f = E\{\tilde{s}^*\tilde{s}\}w_f , \tag{15}$$

so $w_f$ is an eigenvector of $\Phi$, with associated eigenvalue $\lambda=E\{\tilde{s}^*\tilde{s}\}$. If we choose $k>0$, $w_f$ will be the eigenvector associated with the largest eigenvalue of $\Phi$ (the maximum value of $E\{\tilde{s}^*\tilde{s}\}$, which is $2E\{s^2(t)\}$) and if $k<0$, $w_f$ will be the eigenvector associated with the smallest eigenvalue of $\Phi$ (the minimum value of $E\{\tilde{s}^*\tilde{s}\}$).

Assume a desired signal is incident on the array from angle $\theta_d$, and an interference signal from angle $\theta_i$, as shown in Figure 1. Also, assume zero-mean, statistically independent thermal noise of variance $\sigma^2$ is present on each element signal. Then the signals on the array elements are

$$\tilde{x}_1(t) = \tilde{d}(t) + \tilde{i}(t) + \tilde{n}_1(t), \tag{16a}$$

and

$$\tilde{x}_2(t) = \tilde{d}(t-T_d) + \tilde{i}(t-T_i)+\tilde{n}_2(t), \tag{16b}$$

where $\tilde{d}(t)$ and $\tilde{i}(t)$ are the desired signal and interference waveforms,

$$T_d = \frac{\pi}{\omega_o} \sin \theta_d \tag{17a}$$

and

$$T_i = \frac{\pi}{\omega_o} \sin \theta_i \tag{17b}$$

are the interelement propagation time delays for the desired and interference signals, respectively, and $\omega_o$ is the center frequency of the signals. Also,

$$E\{\tilde{n}_i^*(t)\tilde{n}_j(t)\} = \sigma^2\delta_{ij}\,, \tag{18}$$

where $\delta_{ij}$ is the Kronecker delta. In addition, the desired and interference signals are assumed zero mean, and statistically independent of each other and the thermal noise. With these assumptions, the covariance matrix $\Phi$ is found to be

$$\Phi = E\{X^*X^T\} = \sigma^2 I + \begin{bmatrix} R_d(0)+R_i(0) & R_d(-T_d)+R_i(-T_i) \\ R_d(T_d)+R_i(T_i) & R_d(0)+R_i(0) \end{bmatrix} \tag{19}$$

where $R_d(\tau)$ and $R_i(\tau)$ are the autocorrelation functions of $\tilde{d}(t)$ and $\tilde{i}(t)$,

$$R_d(\tau) = E\{\tilde{d}(t+\tau)\tilde{d}^*(t)\}, \tag{20c}$$

and

$$R_i(\tau) = E\{\tilde{i}(t+\tau)\tilde{i}^*(t)\}, \tag{20b}$$

and I is the identity matrix. It is useful to note that $R_d(0)$ and $R_i(0)$ are the incident desired signal and interference powers on each element of the array. Hence we define

$S_d = R_d(0)$ = desired signal power per element

$S_i = R_i(0)$ = interference power per element

and we also define the normalized correlations $\rho_d$ and $\rho_i$:

$$\rho_d = \frac{R_d(T_d)}{R_d(0)} = \frac{R_d(T_d)}{S_d} \tag{21a}$$

$$\rho_i = \frac{R_i(T_i)}{R_i(0)} = \frac{R_i(T_i)}{S_i} \tag{21b}$$

Then the covariance matrix may be written

$$\Phi = \begin{bmatrix} \sigma^2+S_d+S_i & \rho_d^* S_d+\rho_i^* S_i \\ \rho_d S_d+\rho_i S_i & \sigma^2+S_d+S_i \end{bmatrix} \tag{22}$$

The eigenvalues of $\Phi$ are found to be

$$\lambda_{min} = \sigma^2 + S_d + S_i - |\rho_d S_d + \rho_i S_i| \ , \tag{23a}$$

and

$$\lambda_{max} = \sigma^2 + S_d + S_i + |\rho_d S_d + \rho_i S_i| \ . \tag{23b}$$

$\lambda_{min}$ is the minimum value of $E[\tilde{s}^*\tilde{s}]$, which results when $k<0$, and $\lambda_{max}$ is the maximum value, for $k>0$. The eigenvectors associated with $\lambda_{min}$ and $\lambda_{max}$ are also easily found. They are, for $\lambda_{min}$,

$$w_f^{min} = \frac{1}{\sqrt{2}} \left( - \frac{\rho_d^* S_d + \rho_i^* S_i}{|\rho_d S_d + \rho_i S_i|}, \ 1 \right)^T \tag{24a}$$

and for $\lambda_{max}$:

$$w_f^{max} = \frac{1}{\sqrt{2}}\left(+\frac{\rho_d^* S_d + \rho_i^* S_i}{|\rho_d S_d + \rho_i S_i|}, 1\right)^T \tag{24b}$$

For each of these final weights, we may compute the array output desired signal, interference and thermal noise powers.

Consider first the desired signal. The desired signal component at the array output, $\tilde{s}_d(t)$, with weight vector $w_f^{min}$, will be

$$\tilde{s}_d(t) = (\tilde{d}(t)\ \tilde{d}(t-T_d))w_f^{min}$$

$$= \frac{1}{\sqrt{2}}\left[\left(-\frac{\rho_d^* S_d + \rho_i^* S_i}{|\rho_d S_d + \rho_i S_i|}\right)\tilde{d}(t) + \tilde{d}(t-T_d)\right] \tag{25}$$

The output desired signal power is then

$$P_d^{min} = \frac{1}{2} E\{\tilde{s}_d^*(t)\ \tilde{s}_d(t)\}$$

$$= \frac{1}{2}\left[1 - Re\left(\frac{S_d|\rho_d|^2 + S_i\rho_i\rho_d^*}{|S_d\rho_d + S_i\rho_i|}\right)\right]S_d \tag{26}$$

Similarly, the output interference signal with $w=w_f^{min}$ is

$$\tilde{s}_i(t) = [\tilde{i}(t)\ \tilde{i}(t-T_i)]w_f^{min}. \tag{27}$$

and the output interference power is

$$P_i^{min} = \frac{1}{2}\left[1 - Re\left(\frac{S_d\rho_d\rho_i^* + S_i|\rho_i|^2}{|S_d\rho_d + S_i\rho_i|}\right)\right]S_i. \tag{28}$$

The output thermal noise power is

$$P_n^{min} = \frac{\sigma^2}{2} \left( |w_1|^2 + |w_2|^2 \right) = \frac{\sigma^2}{2} , \tag{29}$$

in view of the constraint equation (1).

In a similar way, we find that if the weight vector is $w_f^{max}$, the output desired and interference signal powers are

$$P_d^{max} = \frac{1}{2} \left[ 1 + Re \left( \frac{S_d |\rho_d|^2 + S_i \rho_i \rho_d^*}{|S_d \rho_d + S_i \rho_i|} \right) \right] S_d \tag{30}$$

$$P_i^{max} = \frac{1}{2} \left[ 1 + Re \left( \frac{S_d \rho_d \rho_i^* + S_i |\rho_i|^2}{|S_d \rho_d + S_i \rho_i|} \right) \right] S_i \tag{31}$$

The noise power is the same for $w_f^{max}$ as for $w_f^{min}$, since Equation (1) is satisfied in either case:

$$P_n^{max} = P_n^{min} = \frac{\sigma^2}{2} \tag{32}$$

Equations (26), (28)-(32) may now be used to compute the output desired signal-to-interference-plus-noise ratio (SINR) from the array, defined as

$$SINR = \frac{P_d}{P_i + P_n} . \tag{33}$$

It remains only to define the signals $\tilde{d}(t)$ and $\tilde{i}(t)$, so that $\rho_d$ and $\rho_i$ may be calculated.

Let us assume the desired signal is a zero-mean random process with a flat power spectral density over a bandwidth $\Delta\omega_d$ centered at frequency $\omega_o$. Then $R_d(\tau)$, as defined in Equation (20a), is

$$R_d(\tau) = S_d \frac{\sin \frac{1}{2} \Delta\omega_d \tau}{\frac{1}{2} \Delta\omega_d \tau} e^{j\omega_o \tau} \tag{34}$$

If we define $\phi_d$ to be the desired signal interelement phase shift at frequency $\omega_o$,

$$\phi_d = \omega_o T_d = \pi \sin\theta_d, \tag{35}$$

and also define the fractional bandwidth $B_d$ for the desired signal

$$B_d = \frac{\Delta\omega_d}{\omega_o}, \tag{36}$$

then $R_d(T_d)$ may be written

$$R_d(T_d) = S_d \frac{\sin \frac{1}{2} (B_d \phi_d)}{\frac{1}{2} (B_d \phi_d)} e^{j\phi_d}. \tag{37}$$

Hence, from Equation (21a),

$$\rho_d = \frac{\sin \frac{1}{2} (B_d \phi_d)}{\frac{1}{2} (B_d \phi_d)} e^{j\phi_d} \tag{38}$$

Similarly, we assume the interference has a flat power spectral density of bandwidth $\Delta\omega_i$ centered also at $\omega_o$, so

$$\rho_i = \frac{\sin \frac{1}{2} (B_i \phi_i)}{\frac{1}{2} (B_i \phi_i)} e^{j\phi_i}, \tag{39}$$

where

$$\phi_i = \omega_o T_i = \pi \sin\theta_i, \tag{40}$$

and

$$B_i = \frac{\Delta\omega_i}{\omega_o} \quad . \tag{41}$$

For any given values of the signal parameters $S_d$, $\theta_d$, $B_d$, $S_i$, $\theta_i$ and $B_i$, the powers $P_d$, $P_i$, and $P_n$ and the SINR may be calculated from Equations (26), (28)-(33). In the next section, we give the results of such calculations.

RESULTS

Consider first the case where the signal bandwidths $B_d$ and $B_i$ are zero. Then $\rho_d$ and $\rho_i$ in Equations (38) and (39) reduce to

$$\rho_d = e^{j\phi_d} \tag{42a}$$

$$\rho_i = e^{j\phi_i} \tag{42b}$$

Equations (26)-(33) can then be used to compute the array output SINR.

Figure 4 shows a typical plot of output SINR as a function of input SNR (desired signal-to-noise ratio) for several values of INR (interference-to-noise ratio) and for k<0. With k<0, the weight vector is $w_f^{min}$ and the array output power is minimized. In this case, as long as SNR<INR, the array minimizes the output power by devoting its only null to the interference signal. Hence the output SINR is improved over what it would be without the array processing. When SNR>INR, the null moves over to the desired signal and the output SINR drops below 0 dB.

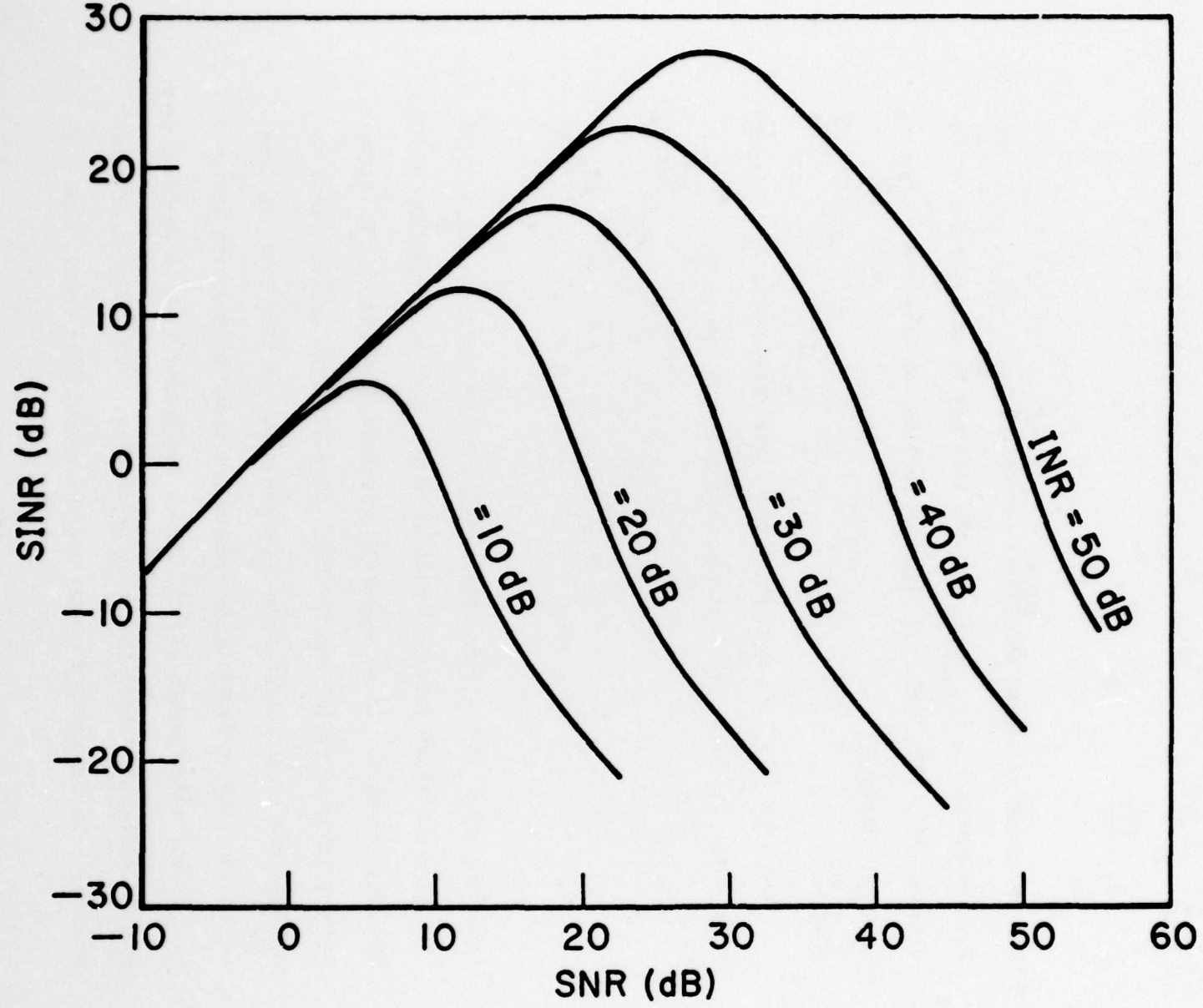


Figure 4. SINR Performance with Power Minimization: $k \triangleleft 0$
$\theta_d = 0^0$, $\theta_i = 50^0$, $B_d = B_i = 0$.

The pattern behavior may be seen in Figure 5 for INR = 40 dB, with SNR = 20 dB, 40 dB and 60 dB. For SNR = 20 dB the null is very close to the interference, and for SNR = 60 dB, it is near the desired signal. Between SNR and 30 dB and SNR = 50 dB, the null moves from one signal to the other. At SNR = 40 dB, the null is approximately half way in between.

Now suppose k>0, so the weight vector is $w_f^{max}$ and the array produces maximum output power. Figure 6 shows the output SINR versus the input SNR for this case. As we would expect, this situation yields a useful output SINR only if SNR>INR.

It is clear from these figures that an SINR>0 dB can be produced for all values of SNR>0 dB except at SNR=INR if the appropriate sign of k can be chosen for each SNR. In a typical design problem, however, the designer has no way of knowing whether an interfering signal will be present, and if so, how strong it will be. Thus, to use this technique one must decide the sign of k while the system is operating. Presumably one would initially set k>0 under the assumption that no interference is present. Then if interference stronger than the desired signal is experienced, the sign of k would be changed. The decision to change the sign of k could be made by a human operator, or, in some cases, with logic circuitry. For example, a communication system using pseudo-noise coding[6] to tag the desired signal[7] must normally acquire code timing before communications can begin. In this situation a threshold voltage is available (e.g., in a delay-lock loop[8]) which indicates whether the timing has been locked. If lockup is not achieved within a certain time, a logic decision can be made to reverse the sign of k.

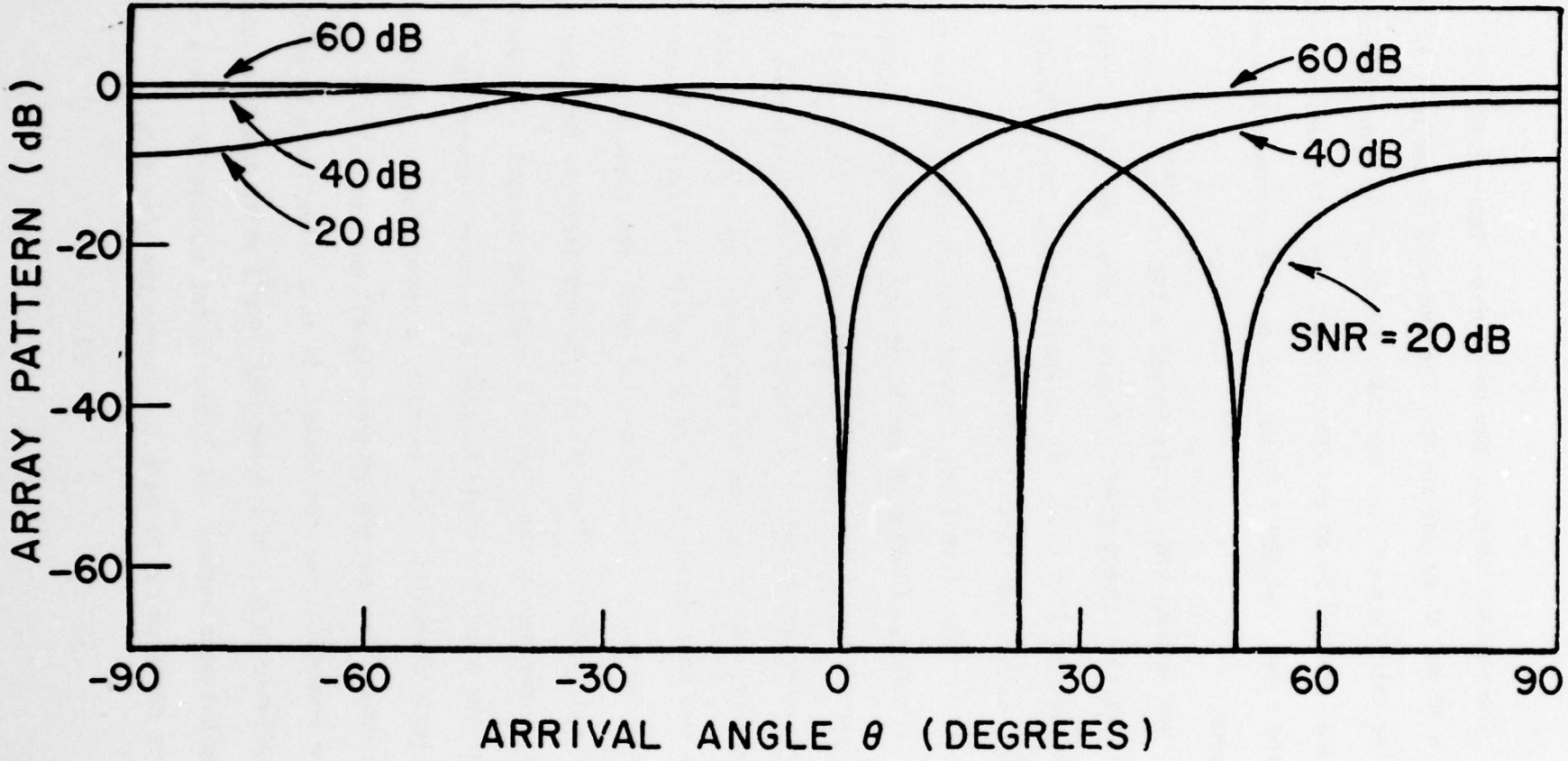


Figure 5. Array Patterns: k<0
$\theta_d=0^0$, $\theta_i=50^0$
$B_d=0$, $B_i=0$
INR=40 dB.

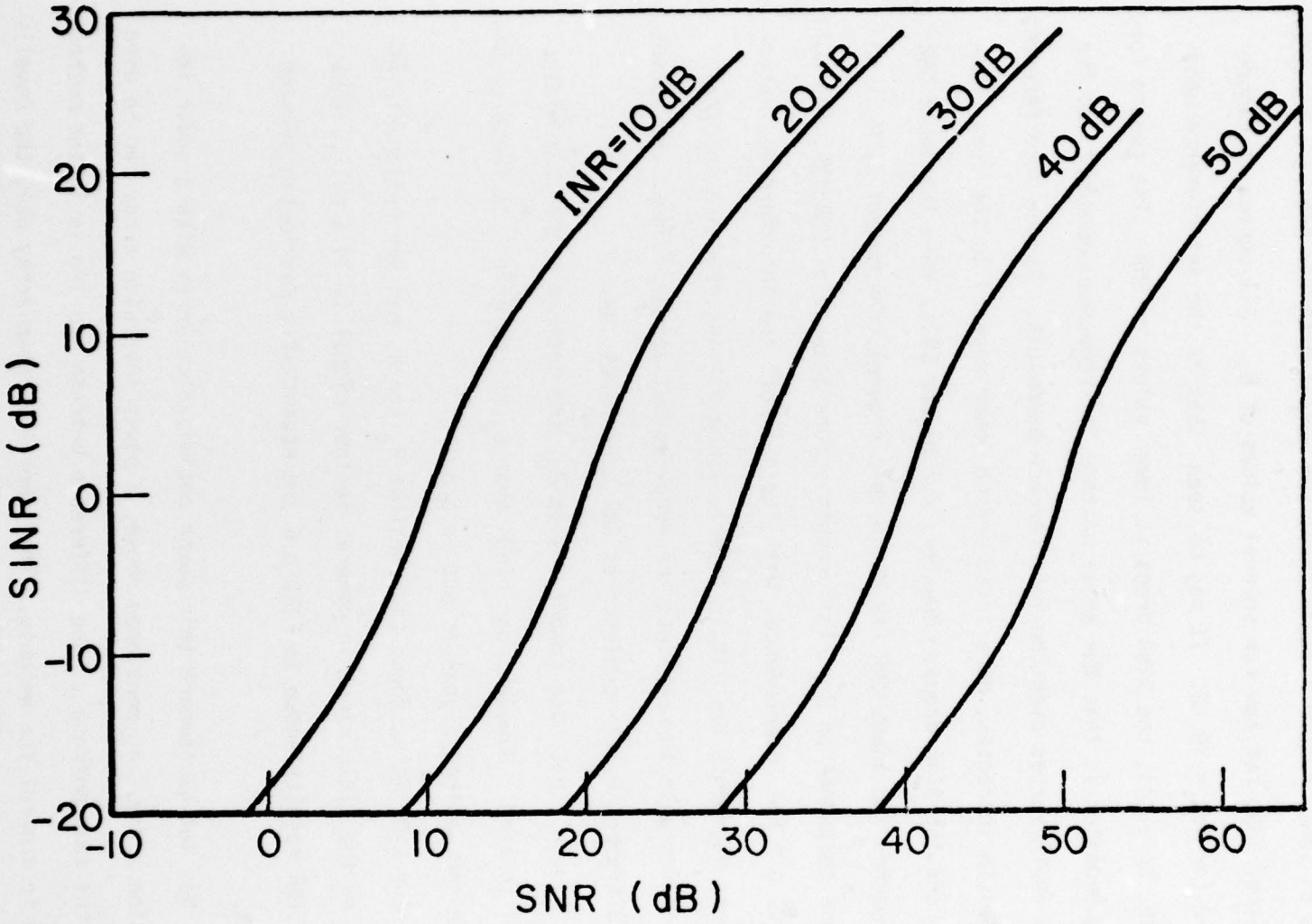


Figure 6. SINR Performance with Power Maximization: k>0
$\theta_d=0^o$, $\theta_i=50^o$, $0 \leq B_d$, $B_i \leq 0.1$.

Now let us consider the effect of bandwidth on the performance of this system. Figure 7 again shows the output SINR for k<0 as a function of input SNR, but now for several values of $B_i$. All curves in Figure 7 are for INR = 40 dB. It may be seen that as the interference bandwidth increases, the SINR drops at lower values of SNR. The reason for this behavior is that the array pattern is frequency dependent, so the null depth varies over the interference bandwidth. As the interference bandwidth increases, more interference power appears in the array output, and the SINR drops. However, for higher SNRs, when the input SNR approaches the input INR (40 dB in this figure), the output SINR is no longer dependent on $B_i$. This result occurs because as SNR→INR, the null shifts off the interference. With the null off the interference, interference bandwidth has little effect, since all interference spectral components pass through into the array output anyway. Thus, the curves for different $B_i$ all coalesce as SNR approaches INR.

Figure 7 has been computed with $B_d$, the desired signal bandwidth, equal to zero. However, one finds that $B_d$ has no effect on these curves, since the desired signal is not in a null.

For k>0, it is found that neither $B_d$ nor $B_i$ has any noticeable effect on the SINR, since in general neither signal is in a null. Thus, the SINR results shown in Figure 6 are essentially unaffected by bandwidth.

Now let us compare this power optimization array with a power inversion array. As mentioned above, a power inversion array can be used for the same purpose[1]. The difference between the two is in the method used to control the weights. The power inversion array uses the Howells-Applebaum feedback loop[2,3].

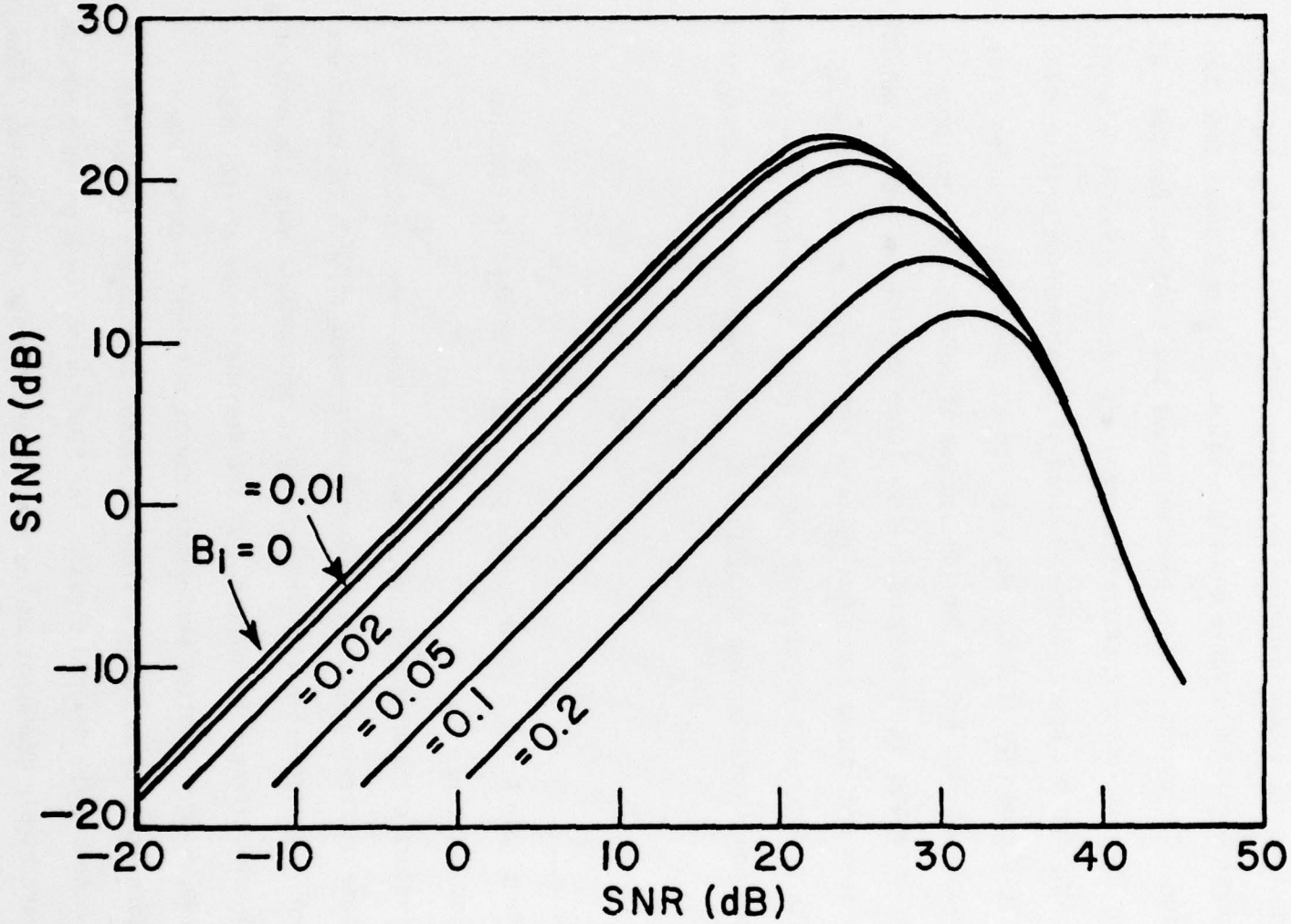


Figure 7. Bandwidth Effects: $k<0$
$\theta_d=0^0$, $\theta_i=50^0$, INR=40 dB
$0 \leq B_d \leq 0.2$.

We find that the power optimization array has the same SINR performance as the power inversion array when SNR<<INR, but has superior performance for SNR's above a certain value. Figure 8 shows this comparison. The output SINR is plotted versus the input SNR for INR = 40 dB for both the power optimization array and the power inversion array. (The SINR for the power inversion array is obtained from Equations (37), (39), (41) and (47) of Reference 1.) For the power optimization array, it is assumed that k<0 if SNR<INR and k>0 if SNR>INR. For the power inversion array, it is assumed that K=.1 for SNR<INR and K=0 for SNR>INR.* It is seen that above a minimum value of SNR (for example, for SNR>15 dB with $B_i$ = 0, or for SNR>20 dB with $B_i$ = 0.1), the output SINR is higher for the power optimization array than for the power inversion array.**

---

*The loop gain K for a power inversion array is defined in Equation (30a) of Reference 1.

**The values of SINR shown here, as well as those shown in Reference 1, assume a steering vector that turns one element off, so the quiescent pattern is omnidirectional. This choice is appropriate when the desired signal arrival angle is unknown. If the desired signal arrival angle is known, however, better performance can be obtained from the power inversion array by choosing a steering vector that points the pattern maximum toward the desired signal. The SINR curves for a power inversion array are highly dependent on the particular steering vector used. (The steering vector is defined in Equation (20) of Reference 1.)

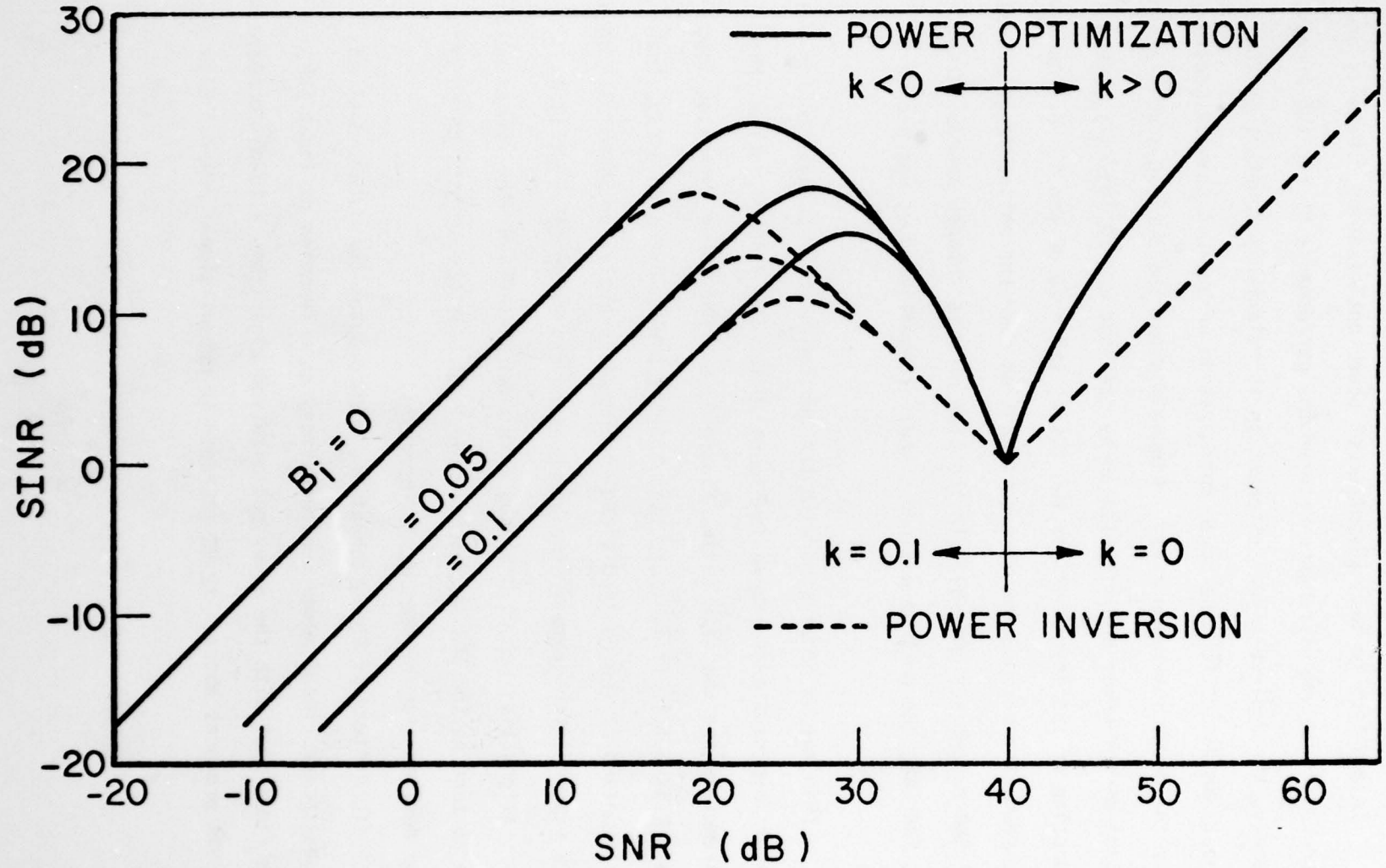


Figure 8. Comparison of Power Optimization and Power Inversion Arrays $\theta_d=0^0$, $\theta_i=50^0$, INR=40 dB, $B_d=0$.

In addition to this advantage of power optimization, there is another interesting difference between the performance of the two arrays. Namely, the desired signal attenuation is relatively constant as the input SNR varies for the power optimization array, but changes greatly for the power inversion array. Figure 9 shows the desired signal attenuation of the power optimization array (defined as $-10 \log P_d/S_d$) as a function of the input SNR for two cases, INR = 20 dB and 40 dB. As may be seen, the attenuation is less than 1 dB over the entire range of values of SNR except for SNR$\tilde{=}$INR. If the sign of k is changed appropriately at SNR=INR, the maximum desired signal attenuation does not exceed 5 dB.

This may be contrasted with the desired signal attenuation for the power inversion array, shown in Figure 10 for INR = 40 dB. (The other parameters are the same as in Figure 9, and the power inversion loop gain K is 0.1.) It is seen that for the power inversion array, the attenuation of the desired signal increases sharply for SNR>0 dB. When SNR = 30 dB, for example, the attenuation has risen to about 45 dB. This attenuation occurs because, with power inversion, the array weights go to zero as the SNR increases above 0 dB. As the weights go to zero, the desired signal attenuation increases.

If, instead of the attenuation, one computes the output desired signal power (input power x attenuation) as a function of input SNR, one finds that with the power optimization algorithm, a 10 dB increase in SNR produces about a 10 dB increase in output signal power. With

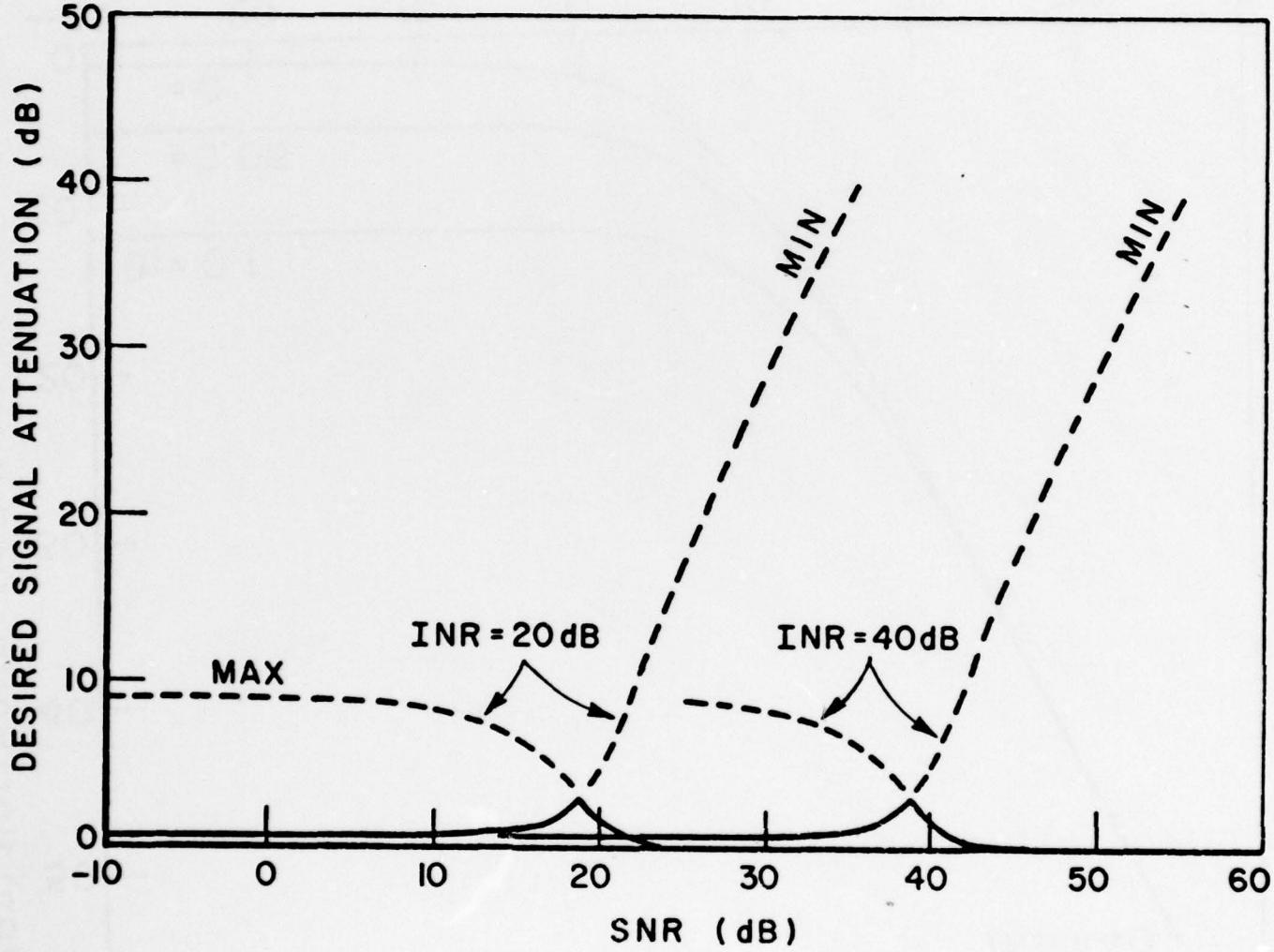


Figure 9. Desired Signal Attenuation (Power Optimization Algorithm) $\theta_d=0^0$, $\theta_i=50^0$, $B_d=B_i=0$.

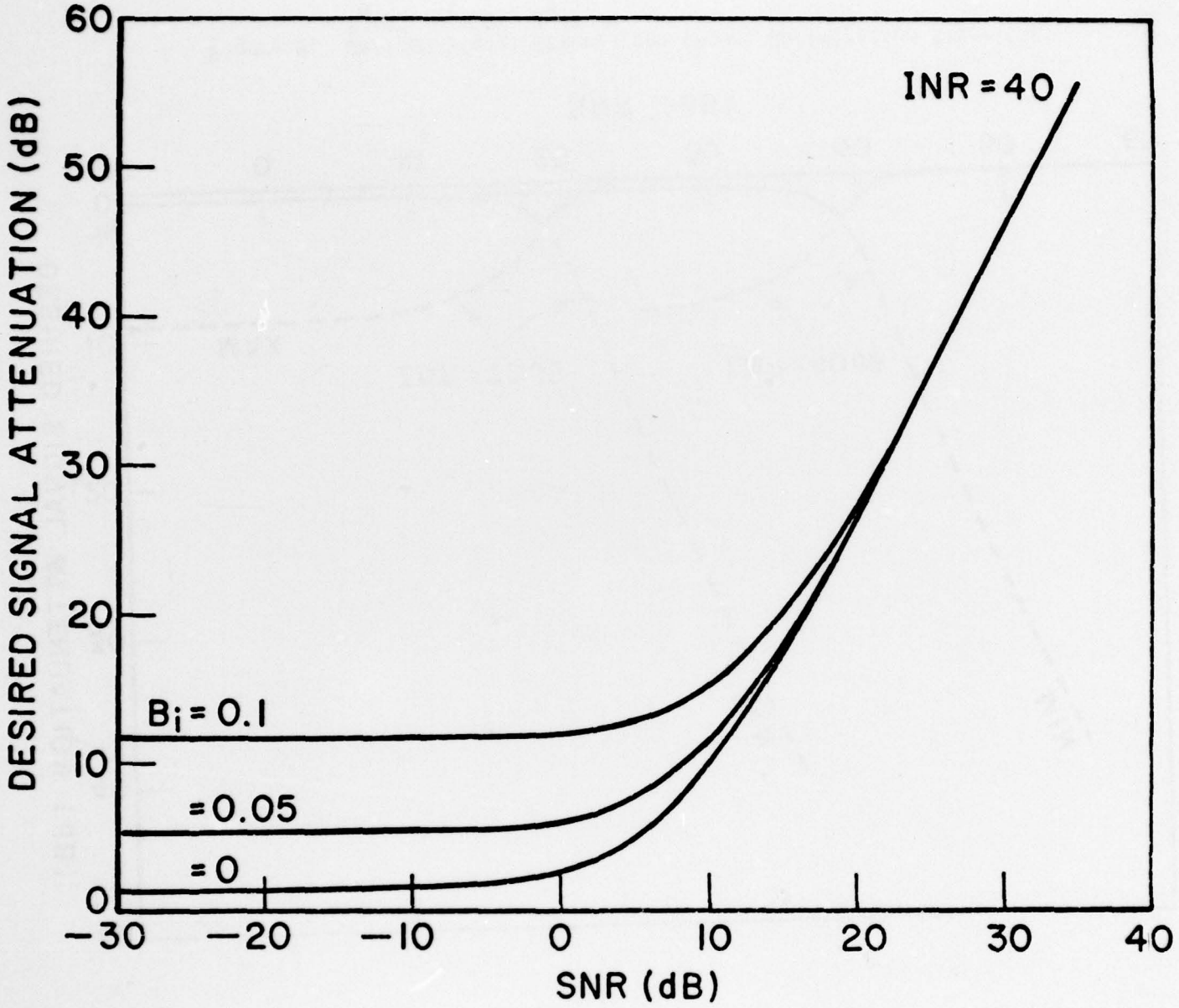


Figure 10. Desired Signal Attenuation (Power Inversion Array) $\theta_d=0^0$, $\theta_i=50^0$, $B_d=0$, K=0.1.

the power inversion array, a 10 dB increase in SNR produces a 10 dB decrease in output power. I.e., the trend is opposite with the two algorithms. It appears that in either case AGC will be necessary at the array output.

## CONCLUSIONS

This paper has shown how a power optimization algorithm may be used with a 2-element array to protect a desired signal from a single interference signal. With this technique the array weights are chosen to minimize or maximize the total array output power, subject to the constraint $\sum_{i=1}^{2} (w_{I_i}^2 + w_{Q_i}^2) = 1$. Output power is to be minimized if SNR<INR and maximized if SNR>INR. The optimum weights are obtained from the iterative algorithm in Equation (3) or with continuous control loops as shown in Figure 2.

An array based on this concept is able to produce a favorable output SINR from the array under most conditions. It is necessary, however, that the sign of the loop gain k be chosen negative if SNR<INR and positive if SNR>INR. Typical curves of output SINR obtained with this technique are shown in Figures 4, 6 and 7. The performance appears to be better than that of a power inversion array with an omnidirectional quiescent pattern, except when the input SNR is weak, in which case the two techniques perform equally well.

REFERENCES


1. R. T. Compton, Jr., "The Power Inversion Array - Concept and Performance," IEEE Trans., AES-15, 5 (September 1979).
2. P. W. Howells, "Explorations in Fixed and Adaptive Resolution at GE and SURC," IEEE Trans., AP-24, 5 (September 1976), 575.
3. S. P. Applebaum, "Adaptive Arrays," IEEE Trans., AP-24, 5 (September 1976), 585.
4. H. H. Al-Khatib and R. T. Compton, Jr., "A Gain Optimizing Algorithm for Adaptive Arrays," IEEE Trans., AP-26, 2 (March 1978), 228.
5. J. Dugundji, "Envelopes and Preenvelopes of Real Waveforms," IRE Trans., IT-4, 1 (March 1958), 53.
6. J. J. Stiffler, Theory of Synchronous Communication, Prentice-Hall, Inc., Englewood Cliff, New Jersey, 1971; p. 178.
7. R. T. Compton, Jr., "An Adaptive Array in a Spread-Spectrum Communication System," Proc. IEEE, 66, 3 (March 1978), 289.
8. J. J. Spilker, Jr., "Delay-Lock Tracking of Binary Signals," IRE Trans., SET-9, (March 1968), 1.